

Detection of the Post-Earthquake Damage in Mamuju Regency in January 2021 Using Sentinel-1 Satellite Imagery

Zulfha Diya Nur Ardzilla

Geomatics Technology Diploma 3
Program, Politeknik Pertanian Negeri
Samarinda, Samarinda, 75131
zulfadiya@gmail.com

Nia Kurniadin*

Geomatics Technology, Politeknik
Pertanian Negeri Samarinda,
Samarinda, 75131
niakurniadin@politanisamarinda.ac.id

*Corresponding author

F. V. Astrolabe Sian Prasetya

Geomatics Technology, Politeknik
Pertanian Negeri Samarinda,
Samarinda, 75131
astrolabesp@politanisamarinda.ac.id

Romansah Wumu

Geomatics Technology, Politeknik
Pertanian Negeri Samarinda,
Samarinda, 75131
romansah@politanisamarinda.ac.id

Dawamul Arifin

Geomatics Technology, Politeknik
Pertanian Negeri Samarinda,
Samarinda, 75131
dawamularifin@politanisamarinda.ac.id

Shabri Indra Suryalfihra

Geomatics Technology, Politeknik
Pertanian Negeri Samarinda,
Samarinda, 75131
shabri.indra@politanisamarinda.ac.id

 Submitted: 2023-05-25; Accepted: 2023-06-08; Published: 2023-06-25

Abstrak—Friday, January 15 2021 at 02:28:21 Local Time, a tectonic earthquake with a magnitude of 6.2 occurred in Mamuju Regency. The epicenter of the earthquake was on land and at 38 km in depth, 6 km to the northeast of Majene, West Sulawesi Province. This earthquake has damaged buildings such as the West Sulawesi Governor's Office, the Mitra Manakara Hospital, and landslides at several points on Mamuju – Majene highway. The purpose of this research is to determine the post-earthquake damage that occurred in Mamuju Regency and to find out the area that was detected because of the earthquake. By using Sentinel-1 satellite image data and the change detection method from two Sentinel-1 SAR images, ESA SNAP software is used for data processing by using a threshold classification on the images before and after the earthquake, then converting Raster to Vector, Clip according to the boundaries of Mamuju Regency and Layouts using ArcGIS software. The results of this study are the detection of the post-earthquake damage that occurred in Mamuju Regency of 100.64 km² (14.78%) total area of damage detected. This research also obtained post-earthquake damage detection maps.

Kata Kunci—Change Detection, Earthquake, Mamuju Regency, Sentinel-1, Threshold Classification.

I. INTRODUCTION

Indonesia is located in the Ring of Fire that stretches from the islands of Sumatra, Java, Bali, Nusa Tenggara, Sulawesi, and Maluku to Papua. So there is a potential for earthquakes and volcanic eruptions caused by friction from the earth. This has been proven by several large and small earthquakes that have occurred in Indonesia. One of them is an earthquake in Mamuju Regency that occurred in 2021, which is expected to start with a foreshock that

occurred earlier on Thursday, January 14, 2021, at 13:35:49 WIB, with a magnitude of 5.9.

Mamuju Regency is one of the regencies located in West Sulawesi Province, at position 2°8'24" S – 2°57'46" S and 118°45'26" E – 119°47'48" E. Mamuju Regency is bordered by Central Mamuju Regency in the North; South Sulawesi Province in the East, Majene Regency and Mamasa Regency in the South, and the Makassar Strait in the West. Mamuju Regency has an area of 4.954,57 km² with 11 Districts (Badan Pusat Statistik, 2022).

Friday, January 15, 2021, at 01:28:21 WIB, there has been a tectonic earthquake with a magnitude of 6.2 in Mamuju Regency. The epicenter of the earthquake was at a depth of 38 km and was on land 6 km to the northeast of Majene, West Sulawesi Province. The occurrence of this earthquake is thought to have started with the opening earthquake (foreshock) which occurred earlier on Thursday, January 14, 2021, at 13:35:49 WIB, with a magnitude of 5.9. According to data from the Geological Agency, earthquakes caused by ascending faults in the western part of West Sulawesi Province triggered tsunamis in 1982, 1967, 1969, and 1984. These earthquakes resulted in damage to buildings and landslides at several points on the Mamuju - Majene highway. According to BMKG data, earthquake shocks were quite strong in the area around the epicenter of the earthquake and were estimated on the V-VII MMI (Modified Mercally Intensity) scale. This earthquake did not cause a tsunami, because the location of the epicenter of the earthquake was located on land. Based on data on January 17, 2021, at 14.00 WIB, the Operations Control Center for the National Disaster Management Agency (BNPB) reported the number of fatalities due to the M 6.2 earthquake which occurred on Friday, January 15, 2021, at 01.28 WIB or 02.28 local time in West Sulawesi Province to 73 peoples, with details of 64 peoples died in

Mamuju Regency and nine people in Majene Regency. Apart from that, there were 554 injured victims in Majene Regency, including 64 seriously injured, 215 moderately injured and 275 slightly injured. There were 27,850 people displaced in 25 evacuation points spread over Kota Tinggi Village, Lombong Village, Kayu Angin Village, Petabean Village, Deking Village, Mekata Village, Kabiraan Village, Lakkading Village, Lembang Village, and Limbua Village. Meanwhile, in Mamuju District, 189 people were seriously injured or hospitalized and there were five evacuation points in Mamuju and Simboro Districts. Furthermore, there are emergency services at 3 hospitals that are currently active in Mamuju Regency, namely Bhayangkara Hospital, Regional Hospital of West Sulawesi Province, and Mamuju Regency Hospital (BMKG, 2021).

From the explanation above, it can be concluded that earthquakes cause losses, damage to buildings and public facilities, and even death. Accurate information on the damage caused by the earthquake is urgently needed to know the impact caused by the earthquake and is useful for post-earthquake reconstruction to be carried out efficiently as well as material for evaluation in the future. Therefore, through this research, the authors utilize sentinel-1 satellite imagery to detect urban damage caused by earthquakes in Mamuju Regency. SAR image data recorded by the Sentinel-1 satellite which is SAR data in Ground Range Detected (GRD) format with Interferometric Wide Swath (IW) acquisition mode with VV / HH (single polarization) and HH+HV, VV+VH (dual polarization) used in this research. According to (Potin et al., 2016), Sentinel-1 satellite imagery is an image designed and developed by the European Space Agency (ESA) in 2014. Sentinel-1 imagery has three types of products, namely Single Look Complex (SLC) consisting of radar data that has been focused, georeferencing using orbit and altitude data from satellites and available on slant-range geometry, Ground Range Detected (GRD), and Level-2 Ocean (OCN) (Nusantara & Sari, 2022).

The purpose of this study was to determine the damage and area detected after the earthquake in Mamuju District. With this research, the expected results are to find out the damage caused by the earthquake in Mamuju Regency with Sentinel-1 imagery and as material for future review and evaluation.

II. LITERATURE REVIEW

A. Earthquake

Earthquakes are vibrations that occur from within the earth and then propagate to the surface of the earth because of cracks in the earth breaking and shifting violently. Some of the causes of earthquakes can be in the form of earth dynamics (tectonics), volcanic activity, falling meteors, landslides below sea level, and subsurface nuclear bomb explosions (Fan et al., 2019). It is estimated that 500,000 earthquakes are detected in the world every year. As many as 100,000 of them can be felt and 100 of them cause damage. The intensity of the

earthquake is measured based on the vibrations produced by the earthquake, the number varies in each location affected by the earthquake (Rany & Mundilarto, 2021; Yalcin et al., 2020).

The Earthquake Intensity Scale is a scale that states the impact caused by an earthquake. The BMKG Earthquake Intensity Scale was initiated and compiled to accommodate information on the impact of earthquakes based on typical cultures or buildings in Indonesia. This scale is structured more simply with only five levels, namely I – V. The BMKG Earthquake Intensity Scale is expected to be useful in conveying information related to earthquake mitigation and/or quick response to destructive earthquake events. This scale can make it easier for the public to be able to understand the level of impact that occurs due to an earthquake better and more accurately. Table 1 provides information on the BMKG Earthquake Intensity Scale.

Table 1. The BMKG Earthquake Intensity Scale

Scale of BMKG EIS	Color	Descriptions	Scale of MMI	PGA (gal)
I	White	Not Felt Not felt or felt by only a few people but recorded by the device	I-II	< 2.9
II	Green	Felt Felt by many people but does no harm. Hanging lightweight objects swayed and glass windows shook	III-V	2.9-88
III	Yellow	Slight Damage The non-structural parts of the building suffered minor damage, such as hairline cracks in the walls, the roof shifted downwards, and some fell	VI	89-167
IV	Orange	Moderate Damage There were many cracks in the walls of the building, some collapsed, glass shattered. Some of the wall plaster is loose. Most of the roof slides down or falls off. The building structure experienced light to moderate damage.	VII-VIII	168-564
V	Red	Heavy Damage Most of the walls of the permanent buildings collapsed. The building structure suffered heavy damage. Curved railroad.	IX-XII	> 564

Most earthquakes occur at a depth of less than 80 km below the earth's surface. Earthquake is a disaster that cannot be prevented, occurs suddenly, and cannot be predicted accurately with the center location, time of occurrence and location of the center. However, earthquakes can be predicted in the range of time that allows them to occur. Earthquakes can be predicted through several methods (Nur, 2010), ie:

1. Short-range prediction

This prediction takes a relatively short time and includes:

- a. Predict the period between foreshock and mainshock or majorshock and major earthquake.

- b. From the history of earthquakes in Japan, America, China, and Russia, the times varied from 24 hours to more than 1 month.
- c. In fact, many are not successful.
2. Long-range prediction
This prediction takes a relatively long time and includes:
 - a. Studying the major earthquake disaster intervals in the past (cycles).
 - b. Cycles are irregular and precise.

B. The History of Earthquake in Mamuju Regency

Earthquakes in West Sulawesi have occurred for decades before, one of which was a major earthquake that occurred in 1967. West Sulawesi is in the Ring of Fire. Geographically, Indonesia is in the Pacific Ring of Fire, which is a confluence of three world tectonic plates, namely the Indo-Australian Plate, the Eurasian Plate, and the Pacific Plate. Therefore, Indonesia is vulnerable to disasters such as earthquakes, volcanic eruptions, and tsunamis. The big earthquake in West Sulawesi first struck Polman and Majene on April 11, 1967, with a magnitude of 6.9, and caused 64 deaths. Then the earthquake in Mamuju Regency on September 6, 1972, with a magnitude of 5.8, and the earthquake on January 8, 1984, with a magnitude of 7.6. The history of the destructive earthquakes and tsunamis in West Sulawesi is as follows (Mulyawan, 2022):

1. Polman–Majene Earthquake 11 April 1967, the magnitude of 6.3 – 64 Deaths – tsunami.
2. Majene Earthquake February 23, 1969, magnitude of 6.9 – 64 Deaths – tsunami.
3. Mamuju Earthquake 06 September 1972, the magnitude of 5.8 – damaging.
4. Mamuju earthquake on January 8, 1984, magnitude of 6.7 – damaging.
5. North Mamuju Earthquake 16 June 2010, magnitude of 5.3 – damaging.
6. Mamasa earthquake on 05 November 2018, a magnitude of 5.2 – damaging.
7. Central Mamuju Earthquake 28 October 2020, magnitude of 5.3 – damaging.
8. Mamuju – Majene earthquake on January 14, 2021, had a magnitude of 5.9 – damaging.
9. Mamuju – Majene earthquake on January 15, 2021, had a magnitude of 6.2 – damaging.
10. Mamuju earthquake 08 June 2022, magnitude of 5.9 – damaging.

C. Remote Sensing

Remote sensing is the science and art of obtaining information about an object, area or phenomenon through the analysis of data obtained with a tool without direct contact with the object, area or phenomenon being measured or observed (Lillesand & Kiefer, 2004). Remote sensing does not only cover raw data collection activities, but also includes automatic (computerized) and manual (interpretation) data processing. Image interpretation is the act of studying aerial photographs or images with the aim of identifying objects and assessing the importance of these objects. There are three series of

activities required in the recognition of objects depicted in images, namely detection, identification, and analysis. Detection is the observation of the existence of objects, identification is an effort to characterize objects that have been detected using sufficient information, and analysis is the stage of collecting further information (Somantri, 2008).

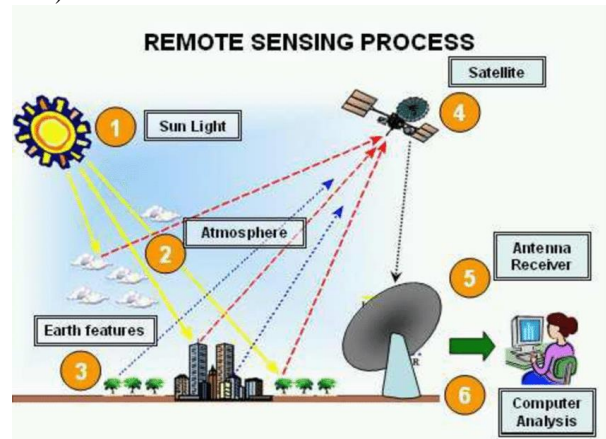


Figure 1. Remote Sensing Components

The types of remote sensing systems that are most frequently encountered are based on the difference in sensors, namely active systems, and passive systems. Passive remote sensing systems are sensors that utilize energy from reflected sunlight or earth energy. Meanwhile, active system remote sensing is a sensor that utilizes energy from the sensor itself (Hussein, 2022).

D. Satellite Orbit System

A satellite is a radio repeater in the air where the satellite system contains transponders, earth stations to control its operations, and users of earth stations equipped with transmitters and receivers from communication lines using the satellite system. A satellite orbiting the earth remains in its position because the centripetal force on the satellite is balanced by the gravitational force from the earth (Kusmaryanto, 2013). An orbit is a regularly repeated path that an object in space takes to get around another object. The types of satellite orbits are differentiated based on the characteristics of the orbital geometry and the movement of the satellite in it, which include:

1. Prograde Orbit

In a prograde orbit, the movement of the satellite in its orbit is in the direction of the earth's rotation with an inclination angle of 0°–90°, calculated counterclockwise at the ascending node, from the equator to the orbital plane (Figure 2).

Prograde: $0 < i < 90$



Figure 2. Prograde Orbit

2. Retrograde Orbit

In retrograde orbit, the movement of the satellite in its orbit is in the opposite direction to the earth's rotation with an inclination angle of 90° - 180° , calculated anticlockwise at the ascending node, from the equator plane to the orbit plane (Figure 3).

Retrograde: $90 < i < 180$



Figure 3. Retrograde Orbit

3. Polar Orbit

Polar-orbiting satellites are very useful for observing the Earth's surface. Because the satellite orbits in a North-South direction and the Earth rotates in an East-West direction, polar-orbiting satellites will eventually be able to sweep across the Earth's surface. A polar-orbiting satellite has an inclination of 90° (Figure 4).

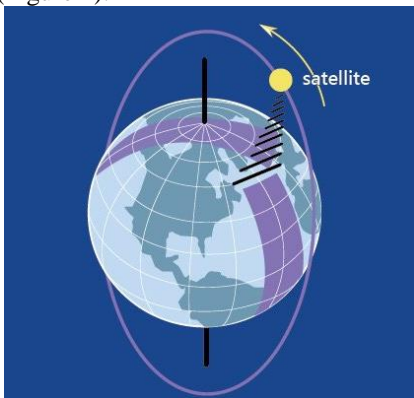


Figure 4. Polar Orbit

4. Geostationary Orbit

In a geostationary orbit, the satellite appears to be stationary from a point on the earth's surface. Geostationary Earth Orbit (GEO), is a circular orbit that is 35,786 km (22,236 miles) above the Earth's equator and follows the direction of Earth's rotation. An object in this orbit will have an orbital period equal to that of Earth's rotation, making it appear motionless, in a fixed position in the sky, to an observer on Earth. Communications and weather satellites are often in geostationary orbits, so that the antennas of the satellites communicating with them do not have to move to track them, but can point permanently at the position in the sky where they are. Only Equatorial orbit (inclination angle of 0°) can be geostationary orbit (Figure 5).

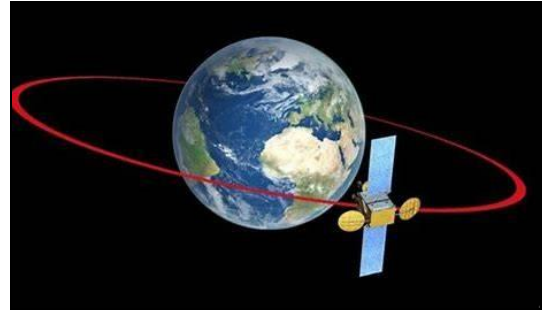


Figure 5. Geostationary Orbit

5. Sun-Synchronous Orbit

In a Sun-Synchronous orbit, the satellite always intersects the direction of the earth's rotation with an inclination angle of 98.2° and an orbital height of 705 km from the earth's surface (Figure 6) (Sergieieva, 2023).

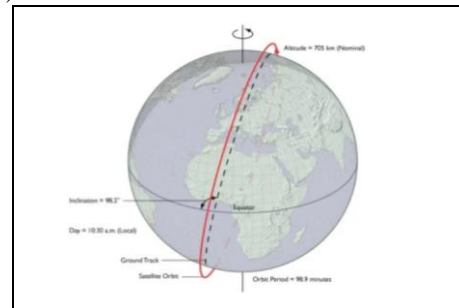


Figure 6. Sun-Synchronous Orbit

Orbital vertices are the two points where an orbit intersects a certain reference plane. An orbit that is not inclined or parallel to the reference plane has no orbital vertices. For satellites that orbit around the earth between the atmospheres with a low inclination angle, the plane that is used as a reference is the plane of the earth's equator or is called the equatorial orbit. Satellite paths that penetrate the equatorial plane at two points are known as Ascending and Descending Nodes (Siregar, 2017).

E. Sentinel-1 Imagery

According to (Potin et al., 2016), Sentinel-1 satellite imagery is an image produced by the Sentinel-1 satellite designed and developed by the European Space Agency (ESA) in 2014. Sentinel-1 imagery has three types of products, namely Single Look Complex (SLC), Ground Range Detected (GRD), and Level-2 Ocean (OCN). The SLC product consists of focused radar data, georeferencing using orbit and altitude data from its satellites, and available slant-range geometry. In this product, the phase information is still available. The GRD consists of focused, multi-looked SAR data that has been projected at ground range using an ellipsoid model such as the WGS84. The ground range coordinates are the slant range coordinates that are projected into the earth's ellipsoid. The pixel value only represents magnitude and has lost phase information. As a result, the GRD product almost has a square pixel resolution with reduced speckles and has an impact on reducing the spatial

resolution of the image (Bashiir & Kurniadin, 2021; Mullissa et al., 2021).

Sentinel was launched on April 3, 2014 carrying an active C-band SAR (Synthetic Aperture Radar) sensor consisting of two satellites, Sentinel-1A and Sentinel-1B, which orbit the pole in tandem 180° apart. Each satellite can perform a repeat cycle every 12 days. With the constellation of the two satellites, Sentinel-1 has a repeat cycle every 6 days. Sentinel-1 has 4 standard operating modes designed for interoperability with other systems, namely:

1. Strip Map (SM) mode records an area of 80 km and a spatial resolution of 5 m x 5 m (single look) and has dual polarization (HH+HV, VV+VH) and single (HH, VV).
2. Interferometric Wide Swath (IW) records over an area of 250 km with the main recorder focused on land and a spatial resolution of 5 m to 30 m (single look) and has dual (HH+HV, VV+VH) and single polarization.
3. Extra-Wide Swath (EW) records data over an area of 400 km with a resolution of 20 m to 40 m and has dual (HH+HV, VV+VH) and single (HH, VV) polarization. EW is the same as IW which uses the TOPSAR technique to obtain data over a large area using five sub-swaths.
4. The Wave (WV) mode picks up data over an area of 20 km x 20 km with a resolution of 5 m x 5 m every 1000 km along the orbit and there are the same two incidence angles on the recorder every 200 km (ESA, 2018; Potin et al., 2016).

The C-band sensor from the Sentinel-1 Satellite Imagery carries two types of polarization VV and VH. VV polarization is the propagation of radar signals emitted and received by sensors vertically toward the aircraft. C-Band has a frequency range between 4 – 8 Hz with a wavelength of 3.75-7.5 cm which can penetrate clouds and rain, so the recording results are free from weather disturbance and can operate day and night, so it is good for various applications in Indonesia which is where the optical image data is often covered by clouds. The intensity of the image is determined by the strength of the backscatter as a function of time. The intensity will be higher if the backscatter strength is high with a low time delay (Bariguna, 2008). As for the land cover backscatter values from the results of the interpretation carried out by the polarization composite of the red channel VV+VH, the green channel VH, the blue channel VV/VH, the backscatter values for the six land covers that can be interpreted are as in Table 2.

Table 2. Land Cover Backscatter Value

Pixel Number	VV Polarization	VH Polarization	Types of Land Cover
4084	0.54028	0.02032	Building
4876	0.00670	0.00277	Open Land
4608	0.29488	0.09840	Forest
3881	0.18373	0.01961	Bush
4819	0.20268	0.05996	Shrubs
3039	0.09605	0.02473	Rice field

From Table 2, the VH polarization has a high backscatter value for forests and shrubs, where land cover with tall vegetation has a greater backscattering reflection, while the VV polarization has a high backscatter value for non-vegetated land cover values such as buildings but not with for open land (Ariyantoni & Rokhmana, 2020). The characteristics of Sentinel-1 imagery in the IW (Interferometric Wide Swath) Recording Mode used in this study can be seen in Table 3.

Table 3. Sentinel-1 Characteristics in Interferometric Wide Swath (IW) Recording Mode

Num.	Characteristic	Information
1	Swath Width	250 km
2	Incidence Angle Range	29.1° – 46.0°
3	Azimuth Resolution	20 m
4	Ground Range Resolution	5 m
5	Azimuth and Range Looks	Single
6	Polarization Options	Dual HH+HV, VV+VH Single HH, VV
7	Maximum Noise Equivalent Sigma Zero (NESZ)	-22 dB
8	Radiometric Stability	0.5 dB (3σ)
9	Radiometric Accuracy	1 dB (3σ)
10	Phase Error	5°

F. Synthetic Aperture Radar (SAR)

SAR is one of the techniques in remote sensing active sensors that use microwaves through the electromagnetic spectrum. SAR is one of the working systems of the radar which is useful for increasing the resolution of RADAR imagery (Bashiir & Kurniadin, 2021).

SAR uses a side-looking radar system that simulates a relatively large antenna and aperture and this can produce high-resolution remote sensing images. SAR can record information on the surface of the earth during the day and night. SAR emits its own energy without depending on energy from the sun, so SAR can be operated day or night and can be used in all weather conditions because the microwave wavelength can penetrate clouds, rain, and smoke. The radar is sensitive to the roughness of the irradiated surface. SAR can penetrate a very dense canopy of vegetation, in contrast to the usual image capabilities, SAR recorders are obtained using an active sensor system. Passive sensors only receive reflections from objects and depend on the presence of the sun or other heat sources, while active sensors emit their own energy radiation to obtain reflections from these objects. Other examples of active sensors are Radar, SAR, and LiDAR. SAR can penetrate clouds and several other objects because the resulting wavelength is longer than the usual optical waves (visible band) and is affected by the canopy structure, besides that the way the radar is recorded in a sideways (side-looking radar) affects the radar's ability to record various objects (Puteri, 2020).

The SAR system makes it possible to observe the same object at different angles with a tilt of 23°. Observations made on the earth's surface obtained a combination of the movement of satellites orbiting along the meridians to the poles and the earth's rotation in the quaternary plane. The SAR system is capable of continuous line imaging so that

it can operate in line mode with a sweep width limited by the system on the satellite. In this case the SAR satellite observes obliquely downwards and indirectly below, therefore when it is in orbit up to the north (ascending) the satellite observes from the west and when the orbit descends to the south (descending) the satellite observes from the east. In moving westward, if the satellite observes in orbit rising to the north (ascending), the surface moves close to the satellite and otherwise, if the satellite observes in orbit descending to the south (descending), the surface moves away from the satellite. This is the reason why the images produced by SAR in the same area but with different observation orbits ascending or descending can look different (Tarikhi, 2012).

III. METHOD

A. Research Location

The location that is the object of this research is Mamuju Regency, West Sulawesi Province (Figure 7). Data processing was performed at the Geomatics Laboratory of the Geomatics Technology Study Program, Agricultural Polytechnic of Samarinda.

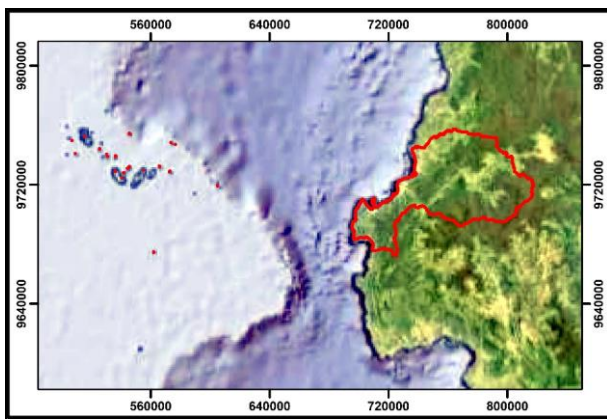


Figure 7. Research Location (50S Zone UTM Projection)

B. Data and Equipment

Administrative boundary data for Mamuju Regency sourced from the Geospatial Information Agency and Sentinel-1 imagery downloaded from the Copernicus Open Access Hub was used in this research. The details of the Sentinel-1 image data used are shown in Table 4.

Table 4. Sentinel-1 Image Data Used in Research

File name	Size	Time
S1A_IW_GRDH_1SDV_20210110 T214324_20210110T214349_036081 _043AAB_1709.SAFE	1,6 GB	2021-01-10 T21:43:24.609Z
S1B_IW_GRDH_1SDV_20210116 T214300_20210116T214300_20210116 T214325_025185_02FFAA_8332.SAFE	1,59 GB	2021-01-16 T21:43:00.416Z
S1B_IW_GRDH_1SDV_20210116 T214235_20210116T214300_025185 _02FFAA_CEFC.SAFE	1,59 GB	2021-01-16 T21:42:35.415Z

The ESA SNAP software is used to process Sentinel-1 images to obtain a combination of threshold classification

values in images before and after an earthquake. Then the ArcGIS software for Raster to Vector conversion, Clip according to the boundaries of Mamuju Regency and Map Layout.

C. Data Collection and Processing

Mamuju Regency Administrative boundary data is collected from the Geospatial Information Agency (<https://tanahair.indonesia.go.id/>), and Sentinel-1 imagery on January 10 2021 and January 16 2021 on the website <https://scihub.copernicus.eu/dhus/> as in Figure 8.

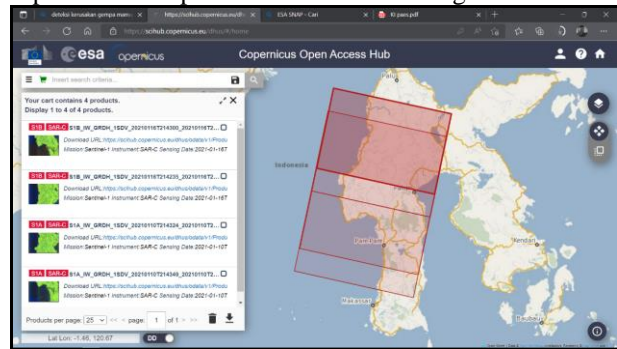


Figure 8. Sentinel-1 Image Data Download Source

By using Sentinel-1 satellite image data and the change detection method from two Sentinel-1 SAR images (before and after earthquake), ESA SNAP software is used for data processing by using a threshold classification on the images before and after the earthquake. Research data processing using ESA SNAP 8.0 software for data before (10 January 2021) and data after (16 January 2021) the earthquake occurred, according to the stages in the following flowchart (Figure 9):

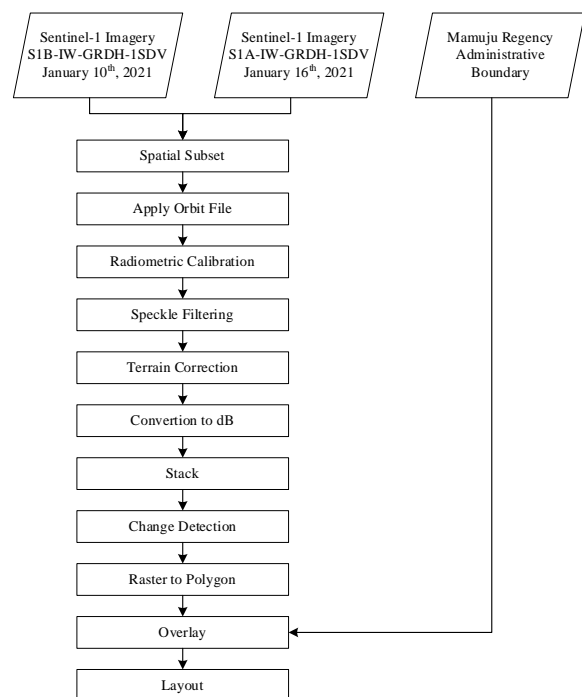


Figure 9. Data Processing Flowchart

Data processing begins by performing a Spatial Subset from View or cropping the Sentinel-1 imagery. This process is carried out to select research areas, with the aim of speeding up processing and selecting VV intensity to give better results.

Apply Orbit File, to update the orbit metadata for Sentinel-1 imagery. The Apply orbit file contains relevant geographic information and this function will be applied to pixel information, including tracking the position and altitude of the Sentinel-1 satellite.

Calibrate is a procedure used to fix the pixel value that truly represents the radar backscattering from the reflected surface. Using VV polarization on the processing parameters and the output is sigma0. Furthermore, Speckle Filtering is performed to improve image quality by removing inherent noise from the radar data.

Terrain Correction, was performed for the geometric correction process. The Sentinel-1 image is still in radar geometry due to the topographic variations of a scene and the tilt of the satellite sensor, distances can be distorted in the image, therefore geometric corrections must be made. Conversion To dB, to better stretch the histogram of the data to a more manageable scale, using the second logarithmic function.

Create a Stack, to compare the difference between before and after by overlapping the two data. To detect the changes that have occurred, the Change Detection process is carried out on the data before and after.

Image cropping according to the boundaries of Mamuju Regency using Clip tools in ArcGIS 10.6.1 software. Then vectorization is carried out using the Raster to Polygon tool, so that overlays, data analysis, and creating Layouts can be done to present data in map form.

IV. RESULTS AND DISCUSSION

The results of SAR data processing in the Ground Range Detected (GRD) format, Interferometric Wide Swath (IW) acquisition mode, VV polarization, and descending orbit on the images on January 10th, 2021, and January 16th, 2021, obtained information and the area of the detected damage caused by the earthquake which different in each sub-district in Mamuju Regency. Information on the distribution of changes and damage is presented in Figure 10.

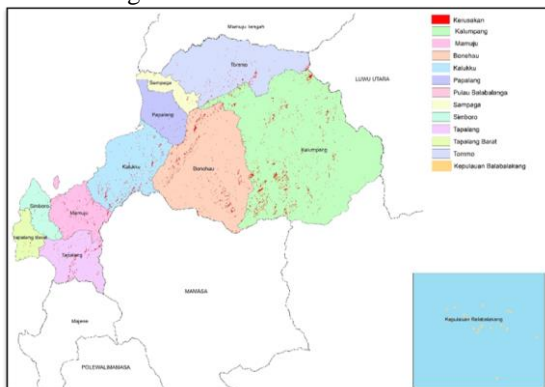


Figure 10. Post-Earthquake Damage Detection Results

Based on some field information sourced from online media which is then used as validation material, there is a discrepancy between the results of Sentinel-1 image data processing and conditions in the field. Some of the damaged areas were not detected even though the actual conditions in the field were damaged. Some sample points that match the results of detection and damage in the field include the Office of the Governor of West Sulawesi Province, Maleo Town Square, Manakarra Stadium, shop buildings, and residents' houses (Figures 11 to 15). As for buildings that were not detected but suffered damage in the field, namely D'Maleo Hotel, Mamuju Police Dormitory, and Mitra Manakarra Hospital (Figure 16 to 18).



Figure 11. Damage Detected at Governor's Office



Figure 12. Damage Detected at Maleo Town Square



Figure 13. Damage Detected at Manakarra Stadium



Figure 14. Damage Detected at Shop Building



Figure 15. Damage Detected at Residents' Houses



Figure 16. No Damage Detected at D'Maleo Hotel



Figure 17. No Damage Detected at Mamuju Police Dormitory



Figure 18. No Damage Detected at Mitra Manakarra Hospital

If there is a discrepancy between the results of Sentinel-1 image data processing and the conditions in the field above, it is necessary to carry out similar research using higher resolution radar images, then use Sentinel-1 image data with ascending orbits or using a combination of ascending and descending orbits. This can affect the detection results obtained, because there is a possibility that when Sentinel-1 takes objects to Earth using ascending orbits, the surface moves close to the satellite and otherwise if the satellite observes in descending orbit, the surface moves away from the satellite. That is why observations in the same area can appear different. So that further research can use data with different orbits or use other methods to be able to detect damage as a whole and the results of damage detection are the same as conditions in the field.

There are several other possibilities why no damage was detected in several places that suffered severe damage in the field, one of which is the possibility that Sentinel-1 imagery has weaknesses related to the strength and weakness of the interaction of wavelengths to an object (sensitivity) either to surface roughness or to changes in height. Several buildings were not badly damaged, such as collapsing or the building only had cracks, so Sentinel-1 imagery did not detect the changes that had occurred. The movement of the ground caused the ruins of the building to shift so that when the satellite imagery captured the part, it had shifted to the other side.

From the results of the damage detection, information was also obtained on area of the damage from each sub-district. Data on the area of damage detected in each sub-district is presented in Table 5. There are 11 sub-districts

in Mamuju Regency, but only 10 sub-districts have detected damage with different extents. The areas with the widest and narrowest damage detected were Kalumpang sub-District with 49.80 km² and West Tapalang sub-District with 0.52 km² respectively. In Kalumpang sub-District, there was a shock with an IV MMI scale, this earthquake was considered not too strong but the impact of the earthquake was able to damage buildings due to alluvium. The earthquake that occurred in Mamuju Regency is an indication of the city's vulnerability to earthquake disasters, where the Regency's position is quite close to the Makassar Strait Fault.

Table 5. Damage Detected Area Data

Sub-Districts	Area of Sub-District (Km ²)	Area of Detected Damage (Km ²)	
Bonehau	870.02	19.20	(2.21 %)
Kalukku	452.65	12.10	(2.67 %)
Kalumpang	1792.55	49.80	(2.78 %)
Kepulauan Balabalakang	1.47	0.00	(0.00 %)
Mamuju	246.22	4.97	(2.02 %)
Papalang	200.89	0.99	(0.49 %)
Sampaga	110.27	0.63	(0.57 %)
Simboro	132.06	0.78	(0.59 %)
Tapalang	271.63	6.14	(2.26 %)
Tapalang Barat	111.06	0.52	(0.47 %)
Tommo	765.75	5.50	(0.72 %)
Total	4,954.57	100.64	(14.78 %)

V. CONCLUSION

Based on the results of the research that has been carried out, it can be concluded that Sentinel-1 Satellite Imagery is capable of detecting post-earthquake damage by using a change detection method and a threshold classification on the images before and after the earthquake, but in several buildings that were damaged quite badly, no damage was detected and the Balabalakang Archipelago Sub-District did not detect any damage at all. One of the possibilities is that Sentinel-1 imagery has weaknesses related to the strength and weakness of the interaction of wavelengths to an object (sensitivity) either to surface roughness or to changes in height. The total area of the detected damage is 100.64 km² and the percentage of damage is 14.78%. The areas that were detected as damage and the percentage of the area of each sub-district were Bonehau 19.20 km² (2.21%), Kalukku 12.10 km² (2.67%), Kalumpang 49.80 km² (2.78%), Mamuju 4.97 km² (2.02%), Papalang 0.99 km² (0.49%), Sampaga 0.63 km² (0.57%), Simboro 0.78 km² (0.59%), Tapalang 6.14 km² (2.26%), West Tapalang 0.52 km² (0.47%), and Tommo 5.50 km² (0.72%).

REFERENCES

- Ariyantoni, J., & Rokhmana, C. A. (2020). Evaluasi Polarisasi Citra SAR (Sythetic Aperture Radar) Untuk Klasifikasi Obyek Tutupan Lahan. *Elipsoida : Jurnal Geodesi Dan Geomatika*, 3(01), 22–29. <https://doi.org/10.14710/elipsoida.2020.7761>
- Badan Pusat Statistik. (2022). Kabupaten Mamuju dalam Angka 2022. In *BPS Kabupaten Mamuju*.

- Bariguna, D. (2008). *Studi Tingkat Kekerusuhan Air Menggunakan Citra RADAR AIRSAR: Vol. Skripsi*. Institut Pertanian Bogor.
- Bashiir, M. F., & Kurniadin, N. (2021). Deteksi Kerusakan Perkotaan Akibat Gempa Bumi di Kota Palu Menggunakan Data Satelit Sentinel-1. *Buletin Poltanesa*, 22(1), 66–69. <https://doi.org/10.51967/tanesa.v22i1.330>
- ESA. (2018). *Sentinel-1 SAR User Guide*. European Space Agency; European Space Agency. <https://sentinels.copernicus.eu/web/sentinel/user-guides/sentinel-1-sar>
- Fan, X., Scaringi, G., Korup, O., West, A. J., van Westen, C. J., Tanyas, H., Hovius, N., Hales, T. C., Jibson, R. W., Allstadt, K. E., Zhang, L., Evans, S. G., Xu, C., Li, G., Pei, X., Xu, Q., & Huang, R. (2019). Earthquake-Induced Chains of Geologic Hazards: Patterns, Mechanisms, and Impacts. In *Reviews of Geophysics* (Vol. 57, Issue 2). <https://doi.org/10.1029/2018RG000626>
- Hussein, S. (2022). *Komponen Penginderaan Jauh Geospasialis*. <https://geospasialis.com/komponen-penginderaan-jauh/>
- Kusmaryanto, S. (2013). Orbit Satelit. In *Komunikasi Satelit* (Vol. 1, p. 26).
- Lillesand, T. M., & Kiefer, R. W. (2004). *Remote Sensing and Image Interpretation*. Gadjah Mada University Press.
- Mullissa, A., Vollrath, A., Odongo-Braun, C., Slagter, B., Balling, J., Gou, Y., Gorelick, N., & Reiche, J. (2021). Sentinel-1 sar backscatter analysis ready data preparation in google earth engine. *Remote Sensing*, 13(10). <https://doi.org/10.3390/rs13101954>
- Mulyawan, I. (2022). *Rekam Jejak Sejarah Gempa Bumi di Sulbar, Berada di Jalur Ring of Fire, Terjadi Sejak 1967*. *Tribun Sulbar*. <https://sulbar.tribunnews.com/2022/06/09/rekam-jejak-sejarah-gempa-bumi-di-sulbar-berada-di-jalur-ring-of-fire-terjadi-sejak-1967>
- Nur, A. M. (2010). Gempa Bumi, Tsunami Dan Mitigasinya. *Jurnal Geografi*, 7(1). <https://doi.org/10.15294/jg.v7i1.92>
- Nusantara, A. F., & Sari, D. K. (2022). Deteksi Penurunan Muka Tanah Menggunakan Metode Dinsar dengan Data Sentinel -A (Studi Kasus: Wilayah Cekungan Bandung, Tahun 2020-2021). *FTSP Series: Seminar Nasional Dan Diseminasi Tugas Akhir 2022*, 288–294.
- Potin, P., Rosich, B., Grimont, P., Miranda, N., Shurmer, I., O’Connell, A., Torres, R., & Krassenburg, M. (2016). Sentinel-1 Mission Status. *Proceedings of EUSAR 2016: 11th European Conference on Synthetic Aperture Radar*, 1–6. <https://ieeexplore.ieee.org/document/7559246>
- Puteri, S. H. (2020). *Pengenalan terhadap Synthetic Aperture Radar (SAR)*. Medium. <https://sryhandiniputeri.medium.com/pengenalan-terhadap-synthetic-aperture-radar-sar-538bc0e59189>
- Rany, T. D., & Mundilarto, M. (2021). Development of Learning Media for Earthquake Disaster Through Physics Subjects to Improve Problem Solving Ability and Disaster Preparedness. *Jurnal Pendidikan Fisika Indonesia*, 17(2). <https://doi.org/10.15294/jpfi.v17i2.27421>
- Sergieieva, K. (2023). *Types Of Satellites: Different Orbits & Real-World Uses*. EOS Data Analytic. <https://eos.com/blog/types-of-satellites/>
- Siregar, S. (2017). *Fisika Tata Surya* (1st ed.). Penerbit Fakultas Matematika dan Ilmu Pengetahuan Alam ITB. <http://www.fmipa.itb.ac.id>
- Somantri, L. (2008). Pemanfaatan Teknik Penginderaan Jauh Untuk Mengidentifikasi Kerentanan Dan Risiko Banjir. *Jurnal Geografi*, 8(2). <https://doi.org/https://doi.org/10.17509/gea.v8i2.1697.g1148>
- Tarikhi, P. (2012). Insar of Aquatic Bodies. *The International Archives of the Photogrammetry, Remote Sensing and Spatial Information Sciences*, XXXIX-B7(September), 85–90. <https://doi.org/10.5194/isprsarchives-xxxix-b7-85-2012>
- Yalcin, I., Kocaman, S., & Gokceoglu, C. (2020). A CitSci approach for rapid earthquake intensity mapping: A case study from Istanbul (Turkey). *ISPRS International Journal of Geo-Information*, 9(4). <https://doi.org/10.3390/ijgi9040266>